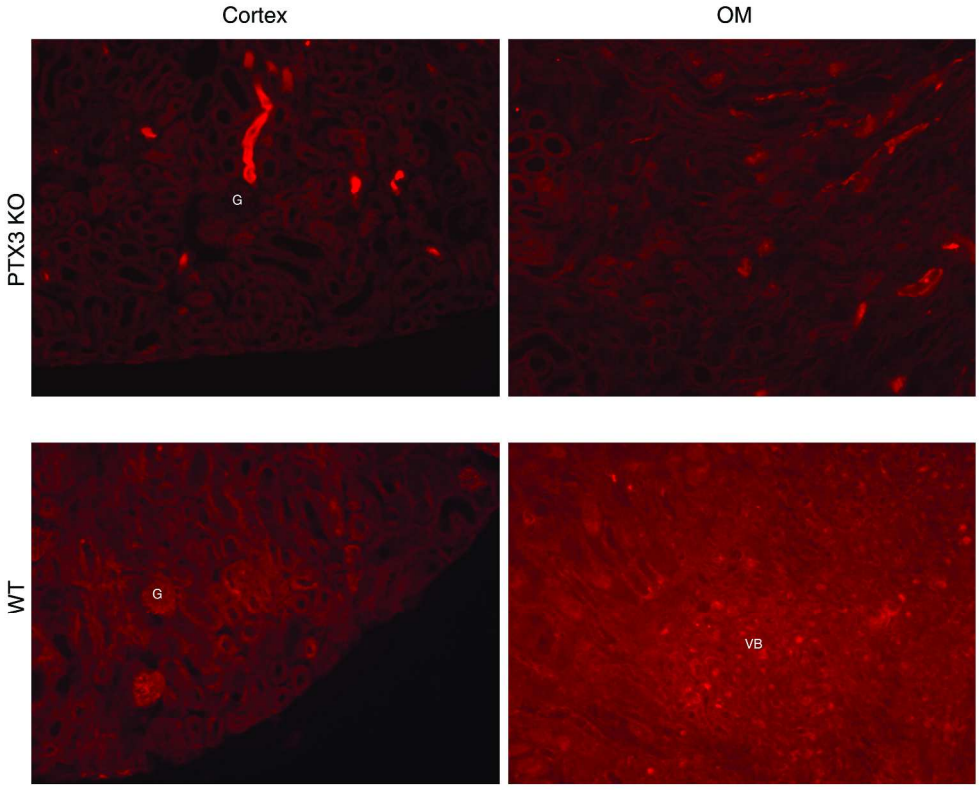

Supplemental Figure 1 PTX3 antibody specificity on IRI kidney sections. Renal pedicles of PTX3 KO and WT mice were clamped for 23min and kidneys were in situ perfused with 4% PFA at 4hr reperfusion. A rat anti-mouse PTX3 mAb was used. On ischemic PTX3 KO kidney sections, no signal was detected on either glomeruli or peritubular structures(x10). However, on ischemic WT kidneys, glomeruli and peritubular structures were positively stained(x10). "G"=glomerulus, "VB"=vascular bundle.
160x134mm (600 x 600 DPI)

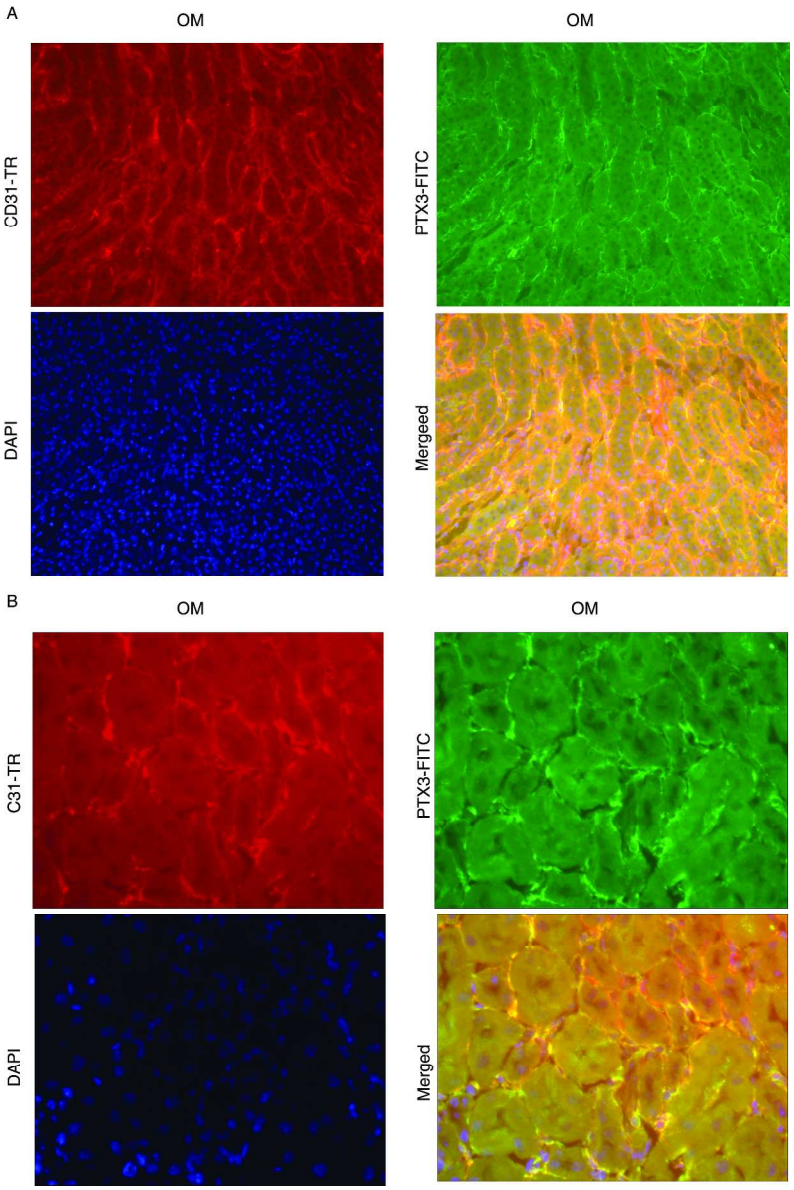

Supplemental Figure2 Double-staining of sham kidney sections shows the co-localization of PTX3 and CD31 on peritubular structures in the OM. Original magnification: (A)x20. (B)x40.
136x199mm (600 x 600 DPI)

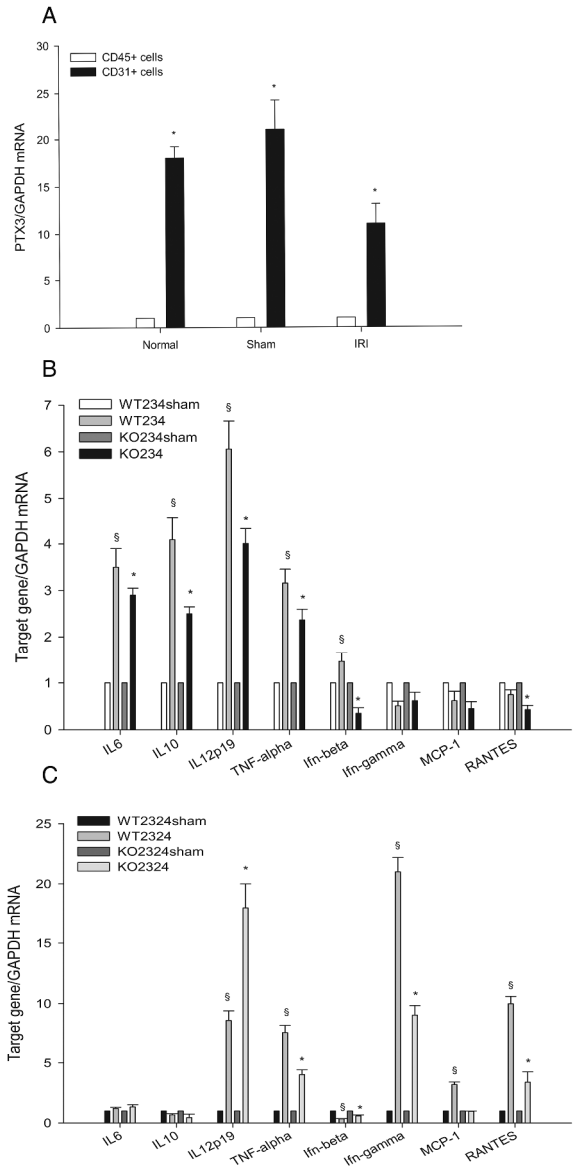

Supplemental Figure 3 CD45+ leukocytes express PTX3. Renal pedicles of WT and PTX3 KO mice were clamped for 23min. CD45+ cells were isolated using Dynabeads from kidney digest at 4hr and 24hr reperfusion. qRT-PCR was performed and data analyzed by comparative Ct method. (A) PTX3 mRNA level was compared between CD31+ cells and CD45+ cells isolated from normal, sham, and ischemic kidneys. Error bars show mean±SEM, n=3 in each group, *P < 0.01 CD31+ versus CD45+cells. (B) Inflammatory gene expression on leukoctyes at 4hr reperfusion. (C) Inflammatory gene expression on leukocytes at 24hr reperfusion. In both "B" and "C", error bars show mean±SEM, n=3 in each group, §P < 0.05 WT IRI versus WT sham, *P < 0.05 PTX3 KO IRI versus KO sham.
99x150mm (1200 x 1200 DPI)

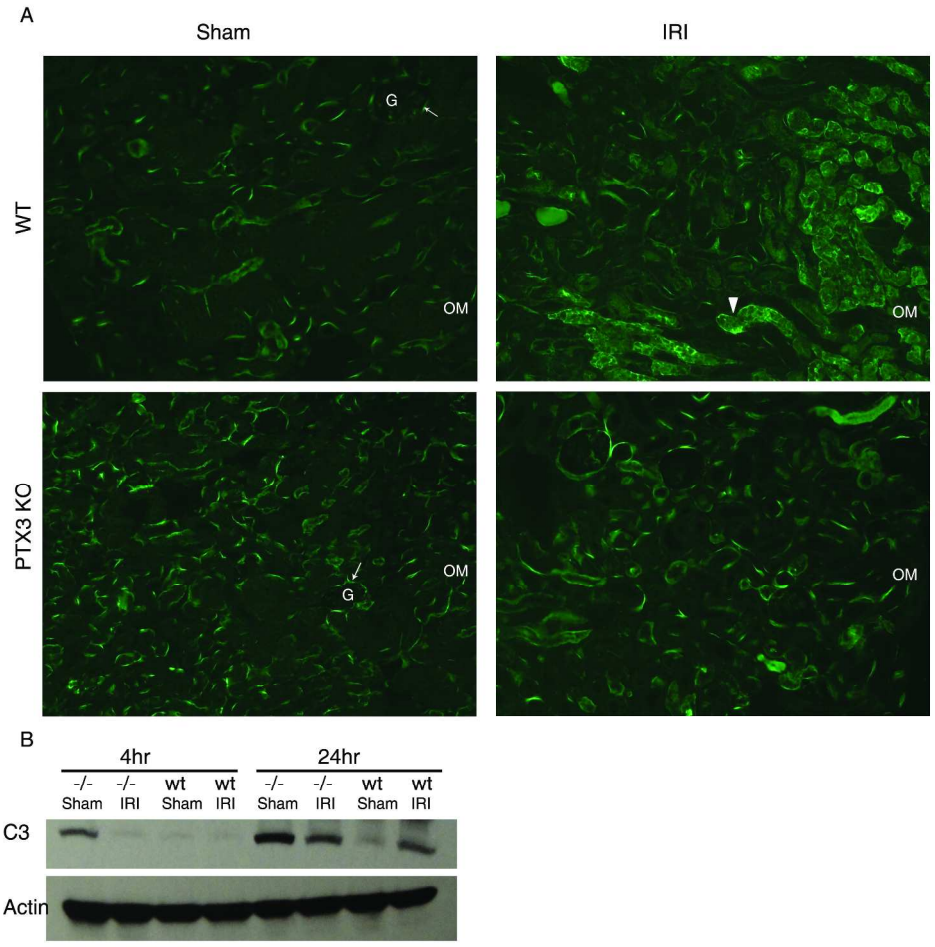

Supplemental Figure 4 Increased C3 in WT ischemic kidneys. Renal pedicles of WT and PTX3 KO mice were clamped for 23min. At 4hr or 24hr reperfusion, kidneys were either in situ perfused with 4%PFA for immunohistology or snap-frozen for protein extraction. A rat anti-mouse C3 monoclonal antibody(Clone RMC11H9, Cedarlane Labs) was used to stain frozen sections from PFA fixed tissues. (A) At 24hr reperfusion, immunohistology showed increased C3 deposition on injured and dead renal tubules on WT kidneys. However it did not increase in KO kidneys(X10). This C3 monoclonal antibody reacts with mouse C3 as well as the breakdown products C3b, iC3b, and C3dg. (B) Western blot of C3 in WT and PTX3 KO kidneys. A goat anti-mouse C3 antibody (Immunology Consultants Laboratory) and a rat anti-mouse C3 antibody were used. β-actin was used for normalization. n=3 in each group. Only the large native C3, not the smaller form that had been activated by C3 convertase, was detectable by Western blot. The data show increased native C3 in the WT, but not the PTX3 KO, kidneys after ischemia.
135x135mm (600 x 600 DPI)

Supplemental Text and Tables

Results

Analysis by Dynabeads shows PTX3 mainly on endothelia; PTX3 on leukocytes plays a less important role during AKI.

In other tissues, PTX3 is expressed by both leukocytes and endothelium. However, by immunohistology, we found PTX3 on endothelium, not leukocytes. Our experiments, using Dynabeads to isolate renal endothelia versus leukocytes confirmed our immunohistology. As shown in Supplemental Figure 3A, by far, the majority of PTX3 is expressed on CD31 endothelia. Thus, we compared the PTX3 mRNA level in harvested CD31+ cells and CD45+ cells. In normal kidneys, the ratio of PTX3 on CD31+ cells vs. non-CD31+ cells was 74±2.2:1, while PTX3 on CD45+ cells vs. non-CD45+ was 3.5±0.8:1. The ratio of PTX3 expression between CD31+ cells and CD45+ cells in normal kidneys, sham kidneys, and IRI kidneys is 18±1.2:1, 21±3.2:1, and 11±2.1:1, respectively (Supplemental Figure 3A). PTX3 is more abundant on endothelial cells. We found that leukocyte IL6, IL10, IL12p19, TNF-α mRNA increased early at 4hr reperfusion in both strains (Supplemental Figure 3B). IFN-γ, MCP-1, RANTES increased at 24hr reperfusion (Supplemental Figure 3C). IFN-β was the only gene that was differentially expressed. At 4hr reperfusion, IFN-β was up by 1.5±0.3 fold in WT, and down by 0.35±0.12 fold in PTX3 KO.

Materials and Methods

DNA microarray. 12 adult male C57BL/10 and TLR4 null C57BL/10ScNJ mice were divided into four groups with three mice clamped for 23 min and three sham mice in each group. At 4hr reperfusion, kidneys were collected, snap-frozen in liquid nitrogen, and stored at -80°C. Samples were homogenized and total RNA was extracted using the RNeasy Midi Kit(Qiagen, Valencia, CA). RNA integrity was checked on Agilent 2100 Bioanalyzer(Agilent Technologies, Santa Clara, CA) with RIN 9.5. Biotinylated cRNA was amplified from 1μg of total RNA using the MessageAmp II-Biotin Enhanced Kit(Ambion, Austin, TX) protocol. Following fragmentation, 15μg of cRNA were hybridized at 45°C for 16 hr on the Affymetrix GeneChip Mouse Genome 430 2.0(Affymetrix, Santa Clara, CA. GeneChips were washed and stained in the Affymetrix Fluidics Station 450 and scanned using the GeneChip Scanner 3000. The data were analyzed with Microarray Suite version 5.0(MAS5.0) using Affymetrix default analysis and global scaling as normalization method. Differential gene expression was interpreted using the GeneSifter Analysis Software(Geospiza, Seatlle, WA).

Table 1 Primers used for mouse genotyping

Gene	Primers
PTX3	5’-ATC CTG CTT TGT GCT CTC TGG T-3’ 5’-CAG CGT GCG TGT AAA CTC AAA G-3’
HPRT(1)	5’-CCT GCT GGA TTA CAT TAA AGC ACT-3’ 5’-GTC AAG GCA TAT CCA ACA ACA AA-3’
MyD88	5’-GTT GTG TGT GTC CGA CCG T-3’ 5’-GTC AGA AAC AAC CAC CAC CAT GC-3’
Tie2Cre	5’-GCG GTC TGGCAGTAAAAACTATC-3’ 5’-GTG AAA CAG CAT TGC TGT CAC TT-3’
Internal control	5’-CTA GGC CAC AGA ATT GAA AGA TCT-3’ 5’-GTA GGT GGA AAT TCT AGC ATC ATC C-3’

Table 2 Primers used for real-time RT-PCR

Gene	Primers
GAPDH	5'-AGG TCG GTG TGA ACG GAT TTG-3' 5'-TGT AGA CCA TGT AGT TGA GGT CA-3'
PTX3	5'-CAT GCG ACT GCC GCC AGG A-3' 5'-TCG TCG GTG GCC TGC AAC A-3'
MyD88(2)	5'-GTT GTG TGT GTC CGA CCG TG-3' 5'-TCT CAA TTA GCT CGC TGG CA-3'
ICAM-1	5'-AGC CAA TTT CTC ATG CCG CAC A-3' 5'-AGC TTT GGG ATG GTA GCT GGA A-3'
VCAM-1	5'-TTC GGT TGT TCT GAC GTG TGC T-3' 5'-AGA GCT CAA CAC AAG CGT GGA T-3'
ESM-1	5'-ATT GCC AGT CGG GCA TAT GTG A-3' 5'-TTC TCT CAC AGC GTT GCC AT-3'
E-selectin	5'-AGC CTG CCA TGT GGT TGA ATG T-3' 5'-AAC GTG CAT GTC GTG TTC CA-3'
P-selectin	5'-TGA ACC ACT GCC AAC CTG TGA A-3' 5'-TGC AGC TGC TGT TGT ACC CAA A-3'
IL6	5'-GGA CCA AGA CCA TCC AAT TCA-3' 5'-CGC ACT AGG TTT GCC GAG TAG-3'
IL10	5'-TGA ATT CCC TGG GTG AGA AG-3' 5'-ACA CCT TGG TCT TGG AGC TT-3'
IL12p19	5'-TGC TGG ATT GCA GAG CAG TAA-3' 5'-GCA TGC AGA GAT TCC GAG AGA-3'
TNF-α	5'-ACG TCG TAG CAA ACC ACC AA-3' 5'-TTG TCC CTT GAA GAG AAC CTG GGA-3'
MCP-1	5'-AAC CTG GAT CGG AAC CAA ATG-3' 5'-GTG CTT GAG GTG GTT GTG GA-3'
IFN-β	5'-ACA CTG CCT TTG CCA TCC AAG A-3' 5'-AAC ACT GTC TGC TGG TGG AGT T-3'
IFN-γ	5'-CTT TAA CAG CAG GCC AGA CA-3' 5'-GCG AGT TAT TTG TCA TTC GG-3'
RANTES	5'-CTC ACC ATA TGG CTC GGA CA-3' 5'-CGA CTG CAA GAT TGG AGC AC-3'
CXCL1	5'-ATG TGT GGG AGG CTG TGT TTG T-3' 5'-ATG TCC AAG GGA AGC GTC AAC A-3'
CXCL4	5'-AGC TGT GTG TGT GTG AAG ACC A-3' 5'-TCC CAT TCT TCA GGG TGG CTA T-3'
NOS3	5'-TTG AGG ATG TGG CTG TGT GCA T-3' 5'-TCA CTT TGG CCA GCT GGT AAC T-3'
FGF2	5'-AAG AGC GAC CCA CAC GTC AAA CTA-3' 5'-AGC CGT CCA TCT TCC TTC ATA GC-3'

References

1.Durlinger AL, Gruijters MJ, Kramer P, Karels B, Kumar TR, Matzuk MM, Rose UM, de Jong FH, Uilenbroek JT, Grootegoed JA, Themmen AP. Anti-Müllerian hormone attenuates the effects of FSH on follicle development in the mouse Ovary. Endocrinology 2001;142(11):4891-4899

2. Hou B, Reizis B, DeFranco AL. Toll-like receptors activate innate and adaptive immunity by using dendritic cell-intrinsic and -extrinsic mechanisms. Immunity 2008;29(2):272-82.